Molecular Crystals and Liquid Crystals

Publication details, including instructions for authors and subscription information:
http://www.tandfonline.com/loi/gmcl20

Molar Mass and Molar Mass Distribution in a Nematic Azobenzene Polymethacrylate: Effect on Optical Recording

L. Andreozzi [a], M. Faetti [a], M. Giordano [a], D. Palazzuoli [a], M. Laus [b] & G. Galli [c]

[a] Dipartimento di Fisica e INFM, Università di Pisa, Pisa, 56127, Italy

[b] Dipartimento di Scienze e Tecnologie Avanzate, Università del Piemonte Orientale, Alessandria, 15100, Italy

[c] Dipartimento di Chimica e Chimica Industriale, Università di Pisa, Pisa, 56126, Italy

Version of record first published: 18 Oct 2010

To cite this article: L. Andreozzi, M. Faetti, M. Giordano, D. Palazzuoli, M. Laus & G. Galli (2003): Molar Mass and Molar Mass Distribution in a Nematic Azobenzene Polymethacrylate: Effect on Optical Recording, Molecular Crystals and Liquid Crystals, 398:1, 97-106

To link to this article: http://dx.doi.org/10.1080/15421400390221457

Mol. Cryst. Liq. Cryst., Vol. 398, pp. 97–106, 2003

ISSN: 1542-1406 print/1563-5287 online
DOI: 10.1080/15421400390221457

Taylor & Francis
Taylor & Francis Group

MOLAR MASS AND MOLAR MASS DISTRIBUTION IN A NEMATIC AZOBENZENE POLYMETHACRYLATE: EFFECT ON OPTICAL RECORDING

L. Andreozzi, M. Faetti, M. Giordano, and D. Palazzuoli
Dipartimento di Fisica e INFM, Università di Pisa, 56127 Pisa, Italy

M. Laus
Dipartimento di Scienze e Tecnologie Avanzate, Università del Piemonte Orientale, 15100 Alessandria, Italy

G. Galli
Dipartimento di Chimica e Chimica Industriale, Università di Pisa, 56126 Pisa, Italy

The mass contents in five samples of a nematic azobenzene polymethacrylate having different molar masses and molar mass distributions were evaluated starting from either Logarithmic Normal (LN) or Zimm-Schulz (ZS) distribution functions. Reliability of these two approaches was verified by comparing the experimental T_g with those predicted (Fox-Flory) on the basis of the LN and ZS mass contents. A birefringent bit was induced in the various samples, and its stability on time was monitored at constant temperature. The optical bit was found to be quite stable at temperatures below that at which conformational disorder was frozen in the nematic phase.

Keywords: azobenzene; molar mass distribution; nematic polymer; optical writing

INTRODUCTION

The combination of photoorientation and thermotropic self-organization [1] represent valuable mechanisms to induce effective alignment in photosensitive azobenzene groups embedded as LC side groups to the polymer main chain. These materials are elegible as potential rewritable high density storage devices [2], whose application however can be prevented by crucial parameters as bit sensitivity and homogeneity at the molecular

This work was supported by the Italian MIUR and INFM (CIPE project P5BW5).

level. In fact, space-time heterogeneities can occur and affect the stability of the photoimprinted information in the azobenzene polymer matrix, whereas the cooperative length of the system can influence the possibility of resolving the minimal bit.

Recently Electron Spin Resonance (ESR) spectroscopy investigations [3] on a polymethacrylate (PMA4) containing azobenzene side groups have allowed to single out a suitable procedure to get a stable, homogeneous polymeric substrate. Following the selected procedure, optical studies on micrometer length scale have confirmed the stability conditions in both unaligned and aligned samples [4]. More recently, substantial advances in nanolithography and high density storage were obtained by performing optical nanowriting and topographic reading with subwavelength resolution on PMA4 [2,5].

Another important parameter from an applicative point of view is the avaibility of as wide as possible stability temperature range. ESR studies [3] permitted the identification of a conformational transition intermediate between T_g and the clearing temperature T_{NI}. This transition temperature was found to depend on the molar mass and molar mass distribution of the polymer sample. Very significantly, this temperature also resulted to represent an upper limit below which the photoinduced recording was stable.

The influence of molar mass of LC polymers on their mesophase structure and transition behaviour is generally well known, and can also affect different physical properties of the polymers, such as responsiveness to external applied fields.

In this work, we intend to elucidate the effects of the molar mass and molar mass distribution on macroscopic and microscopic properties of the azobenzene polymers.

EXPERIMENTAL PART

Materials

The PMA4 under investigation is a polymethacrylate containing the (3-methyl-4′-pentyloxy)azobenzene mesogenic unit connected at the 4-position by an hexamethylene spacer to the main chain [3]. The methacrylate monomer was synthesized following a standard procedure [6]. This was used in five polymerization batches (syntheses S1 to S5) in which the experimental conditions (concentrations of monomer, initiator, and chain transfer agent; polymerization time) were adjusted to yield five PMA4 samples with different molar masses and molar mass distributions. Full experimental details will be given elsewhere.

Characterizations and Measurements

Average molar masses were determined by size exclusion chromatography (SEC) of chloroform solutions with a 590 Waters chromatograph that was equipped with two Shodex KF804 columns and both RI R401 and UV LC75 detectors. Polystyrene standard samples ($M_n = 1.10^3$–5.10^5) were used for calibration.

Differential scanning calorimetry (DSC) measurements were performed with a Perkin-Elmer DSC7 calorimeter calibrated with indium. Before DSC experiments, all the samples were first mantained for 4 h to a temperature above T_{NI}, then cooled to 250 K at a cooling rate of 40 K/min. Immediately after, thermograms were recorded at a heating rate of 10 K/min.

The samples were prepared by the solution casting yielding reasonably homogeneous specimens of about 4 μm of thickness. The optical observations were carried out with a Zeiss Axioplan 2 polarizing microscope connected to a video camera for recording of the images. The sample was placed between two crossed polarizers and an interferometric filter (wavelength center $\lambda = 650.2$ nm and bandwith $\Delta\lambda = 91$ nm) was used to monitor the system without inducing any isomerization cycle. To obtain a small optical spot, the field diaphragm aperture was reduced to the minimum size and the optical filter was removed.

Basic Definitions and Numerical Approaches

The determination of molar mass and molar mass distribution (MWD) of polymers is routinely performed by size exclusion chromatography (SEC) methods [7,8] and great importance is devoted to the interpretation of the experimental data by the use of computer simulations and fit procedures [9–11]. Different theoretical molecular weight distributions can be considered in order to simulate the experimental polymeric MWD. Generally, discrete distributions can be approximated by continuous theoretical functions. The polymerisation process typology [12] and tipical features of statistical functions [13,14] (e.g. logarithmic normal, Poisson, generalized exponential function) can lead to the choice suitable for the various experimental data.

Let $F(x_i)$ be the molar fraction with x_i degree of polymerization (DP); the MWD results to be fully characterized by the moments:

$$\bar{x}_n = \frac{\sum_{i=1} x_i \cdot F(x_i)}{\sum_{i=1} F(x_i)} \quad \bar{x}_w = \frac{\sum_{i=1} x_i^2 \cdot F(x_i)}{\sum_{i=1} x_i \cdot F(x_i)} \quad \bar{x}_j = \frac{\sum_{i=1} x_i^j \cdot F(x_i)}{\sum_{i=1} x_i^{j-1} \cdot F(x_i)} \qquad (1)$$

being $\bar{x}_n$, $\bar{x}_w$, $\bar{x}_j$ the number average degree, the weight average degree and the higher order moments of the distribution respectively. The first four moments $\bar{x}_n$, $\bar{x}_w$, $\bar{x}_3$ (or $\bar{x}_z$) and $\bar{x}_4$ are the principal weight averages

commonly in use. Replacing in all Eqs. (1) the DP x_i with the masses $M_i = x_i \cdot m_0$ (with m_0 molecular weight of the polymeric repeating unit), the number average molecular weight M_n, and the weight average molecular weight M_w are easily calculated. If the MWD of a polymer is determined by SEC, the technique provides a response which is directly proportional to the mass fraction $W(x_i)$ rather than to the fraction number $F(x_i)$. These quantities are connected by the relation:

$$W(x_i) = \frac{x_i \cdot F(x_i)}{\sum_{j=1} x_j \cdot F(x_j)} \tag{2}$$

and the averages M_n, M_w, M_z, M_j may be calculated from the mass distribution:

$$\begin{aligned} M_n &= \frac{\sum_{i=1} W(M_i)}{\sum_{i=1} W(M_i)/M_i} \quad & M_w &= \frac{\sum_{i=1} W(M_i) \cdot M_i}{\sum_{i=1} W(M_i)} \\ M_z &= \frac{\sum_{i=1} W(M_i) \cdot M_i^2}{\sum_{i=1} W(M_i) \cdot M_i} \quad & M_j &= \frac{\sum_{i=1} W(M_i) \cdot M_i^{j-1}}{\sum_{i=1} W(M_i) \cdot M_i^{j-2}} \end{aligned} \tag{3}$$

In order to numerically reproduce the experimental MWDs we adopted in this work the logarithimic normal (LN) [15] and the Zimm-Schulz (ZS) functions, the latter being a generalized exponential function:

$$W_{LN}(M, \bar{M}, \sigma) = \frac{1}{\sqrt{2\pi\sigma^2}} \cdot \frac{1}{M} \cdot \exp\left[-\frac{(\ln M - \ln \bar{M})^2}{2\sigma^2} \right] \tag{4}$$

$$W_{ZS}(M, M_n, \alpha) = \frac{m_0 \cdot \alpha}{M_n \cdot \Gamma(\alpha + 1)} \cdot \left(\frac{\alpha \cdot M}{M_n} \right)^{\alpha} \cdot \exp\left(-\frac{\alpha \cdot M}{M_n} \right) \tag{5}$$

with $\left(\frac{M_w}{M_n} = \frac{\alpha+1}{\alpha} \right)$.

RESULTS AND DISCUSSION

Each PMA4 sample formed a nematic phase between the glass transition (T_g) and clearing (T_{NI}) temperatures (Table 1). The DSC scans relevant to the five investigated different syntheses are reported in Figure 1a. Figure 1b shows an enlarged region pointing to the occurrence of a conformational transition of the polymer backbone at intermediate temperature (T_c) [4].

The rise of the T_g values may denote an increase in the first moments of the MWD or in the content of higher molar mass components. The experimental chromatograms of the different PMA.4 samples are illustrated in Figure 2.

The first four moments of the MWDs and the polydispersity values, evaluated from the experimental data by using Eq. (3), are collected in Table 2. The SEC molar mass data were rather scattered and no clear

TABLE 1 Temperatures of the PMA Syntheses from DSC Experiments

Synthesis	T_g (K)	T_c (K)	T_{NI} (K)
S1	292.0	320.0	353.0
S2	296.0	333.0	351.0
S3	302.5	330.0	353.0
S4	303.0	329.0	354.0
S5	305.0	337.0	357.0

correlation appeared to be possible with the detected DSC results. A better understanding could be achieved by a different careful analysis of the data.

At the lowest order, experimental chomatograms W_{EXP} can be expanded as superposition of two distributions:

$$W_{EXP}(M) = C_1 \cdot W_{LN}(M, \bar{M}_1, \sigma_1) + C_2 \cdot W_{LN}(M, \bar{M}_2, \sigma_2)$$

or

$$W_{EXP}(M) = C_1 \cdot W_{ZS}(M, M_{n1}, \alpha_1) + C_2 \cdot W_{ZS}(M, M_{n2}, \alpha_2)$$

with $C_1+C_2=1$. C_1 and C_2 are the mass fractions of the two polymer species, and W_{LN} and W_{ZS} are the LN and ZS functions, respectively. The best fits of the experimental chromatograms by using the superposition of two LN and two ZS functions are depicted in Figures 3 and 4, respectively.

It should be noted that, for both LN and ZS choices, the superpositions are sufficient to provide very good representation of the experimental data. The physical parameters relevant to Figures 3 and 4 are reported in Tables 3 and 4, respectively.

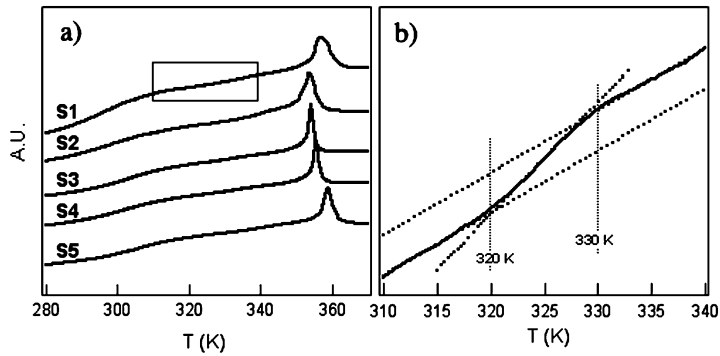

FIGURE 1 DSC curves of the PMA4 samples from S1-S5 syntheses (a) with an enlarged region for the sample from S1 synthesis (b).

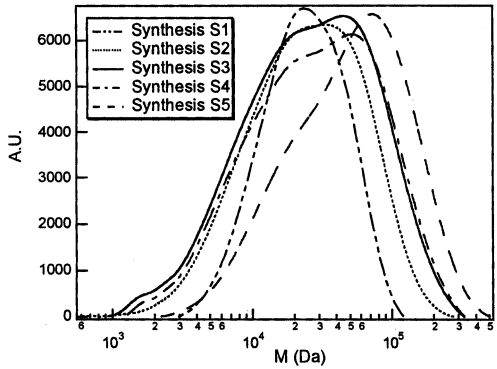

FIGURE 2 Experimental chromatograms of PMA4 samples.

Interestingly, one notes that increased values of T_g correspond to increased values of M_{n1}, the number average molar mass of the higher component, in both in LN and ZS approaches. Moreover, the percentages of heavier polymer component increase in samples from S1 to S5.

In order to test the reliability of these numerical approaches, the comparison between the experimental T_g values and the theoretical ones, is carried out by using the Fox-Flory expression [16] and the Fox rule [17]:

$$T_g(M) = T_{g_\infty} - \frac{M_\infty}{M} \tag{6}$$

$$\frac{1}{T_g} = C_1 \cdot \frac{1}{T_{g1}} + C_2 \cdot \frac{1}{T_{g2}} \tag{7}$$

The results obtained by using LN and ZS are reported in Tables 5 and 6, respectively. The values of T_{g_∞} (and M_∞) evaluated by the LN and ZS approaches resulted to be 324 K (and 878200 g/mol) and 312 K (and 733720 g/mol), respectively.

In both cases there was excellent agreement between experimental and theoretical (Fox-Flory) T_gs, which indeed does not allow one to

TABLE 2 SEC Average Molar Masses and Polydispersity Indices

Synthesis	M_n	M_w	M_z	M_4	M_w/M_n
S1	18600	59006	171238	310412	3.17
S2	15318	35539	64355	93834	2.32
S3	14299	42326	85726	127940	2.96
S4	15705	45873	91773	134571	2.92
S5	29878	72605	130544	186787	2.43

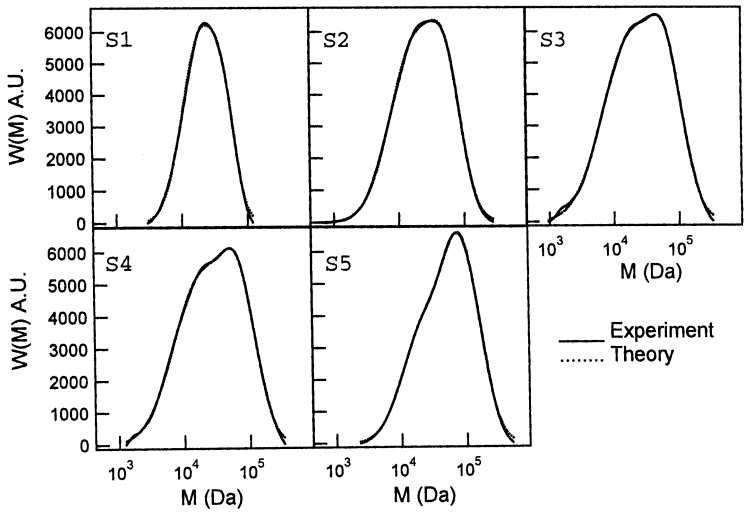

FIGURE 3 Experimental chromatograms and best fits with two LN functions.

discriminate between the two numerical approaches. With this respect, different considerations are necessary. According to Table 4, the values of the mass fraction of the high molar mass component C_1 seem to be overestimated by ZS, reaching as much as 98% in S5. The low molar mass component in S3 and S4 is on the order of the error. In S5 it is even less than

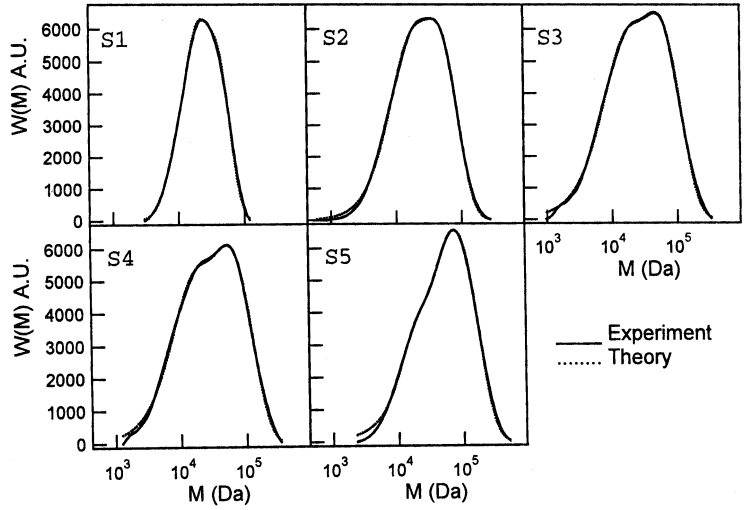

FIGURE 4 Experimental chromatograms and best fits with two ZS functions.

TABLE 3 Fit Parameters Obtained by Using Two LN Functions

	Synthesis				
	S1	S2	S3	S4	S5
C_1	0.16	0.21	0.22	0.29	0.56
$\bar{M}_1$	52500	72700	94000	102900	133000
M_{w1}	48700	64200	80000	85300	107000
M_{w1}/M_{n1}	1.14	1.27	1.35	1.39	1.49
C_2	0.84	0.79	0.78	0.71	0.44
$\bar{M}_2$	31700	44000	57100	50700	42700
M_{w2}	25200	28700	32300	30200	31200
M_{w2}/M_{n2}	1.51	2.22	2.71	2.52	1.85

TABLE 4 Fit Parameters Obtained by Using Two ZS Functions

	Synthesis				
	S1	S2	S3	S4	S5
C_1	0.78	0.91	0.94	0.94	0.98
M_{n1}	37100	42300	48600	53300	74300
α_1	3.47	1.68	1.23	1.25	1.35
M_{w1}/M_{n1}	1.29	1.59	1.81	1.80	1.74
C_2	0.22	0.09	0.06	0.06	0.02
M_{n2}	16000	12800	12300	12300	16200
α_2	3.84	2.59	2.42	2.43	4.86
M_{w2}/M_{n2}	1.26	1.39	1.41	1.41	1.21

TABLE 5 Experimental and Theoretical T_g (LN) Values

Synthesis	S1	S2	S3	S4	S5
T_g^{exp}	292	296	302	303	305
T_g^{th}	292	297	301	301	307

TABLE 6 Experimental and Theoretical T_g (ZS) Values

Synthesis	S1	S2	S3	S4	S5
T_g^{exp}	292	296	302	303	305
T_g^{th}	292	298	301	302	306

the estimated uncertainty, and on the other side, the corresponding anomalously high value of C_1 in S5 is at variance with the possibility of reproducing the physics of the system by a single distribution. It should also be taken into account that ZS is a function with a long tail on the low molar mass side, which was firstly considered in literature to describe the MWD of step-wise polymers [15]. Note that the polydispersity of the ZS high molar mass component is systematically larger than the corresponding LN one. This was because of the necessity of well fitting the tailing in the high molar mass side, which in turn drastically reduced the content of the low molar mass component C_2. Accordingly, we conclude that the overestimation of C_1 was generated by a numerical artifact due to the distinct form of the ZS distribution function. Consequently, we assume that LN approach best represents the molecular mass distribution of the free-radical PMA4 polymer samples.

From Tables 1 and 3, it is seen that the T_c values increase with C_1 and $\bar{M}_1$. This result turns out to be of interest from an applicative point of view. In fact calorimetric, ESR, Longitudinally Detected ESR (LODESR) and optical [4] studies on the S1 sample had proved that the freezing of conformational disorder of the main chain below T_c, driven by the nematic order, allowed us to get stable optical bit even above the T_g.

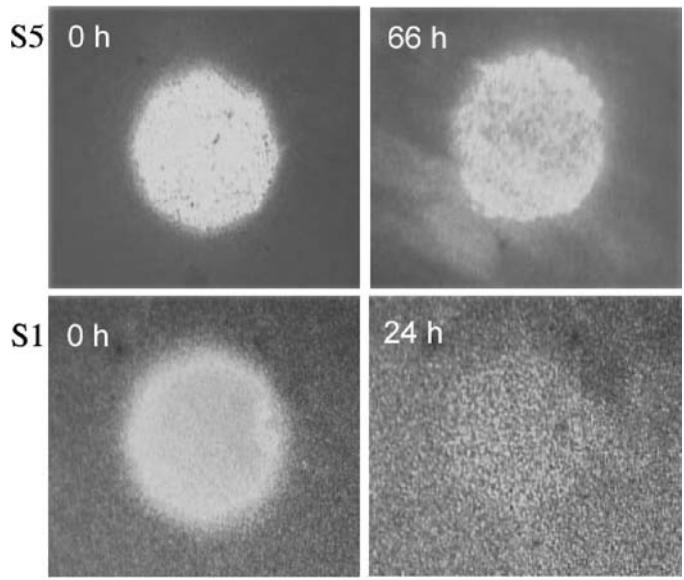

FIGURE 5 (see COLOR PLATE XXXVI) Induced birefringence in PMA4 S1 and S5 samples at 338 K after different times from irradiation (between crossed polarizers at $\pi/4$).

In this work we performed optical writing experiments on S1 and S5 samples, which exhibited very different values of C_1 and $\overline{M}_1$. In Figure 5, the relative stability at 338 K of the optical bit is compared.

Whereas, the optically induced birefringence in the S5 sample remained quite stable over prolonged periods of time, it almost totally vanished in the S1 sample after as short as 24 hours. This finding could be ascribed to the sensibly higher T_c in the former than in the latter sample, consistent with previous results [4]. Thus, the chance of enlarging the working temperature range for optical recording would pass through the synthesis of polymer samples with appropriately high molar mass.

CONCLUSIONS

Careful DSC measurements and molar mass analyses of the polymer samples allow to confirm the stability of the photoinduced birefringence at temperatures below the one at which conformational disorder freezes in the nematic phase. This finding may address one crucial feature of bit stability and suggest prescription of azobenzene polymethacrylates with optimized transition temperatures for information storage.

REFERENCES

[1] Meier, J. G., Ruhmann, R., & Stumpe, J. (2000). *Macromolecules*, *33*, 843.
[2] Patanè, S. Arena, A., Allegrini, M., Andreozzi, L., Faetti, M., & Giordano, M. (2002). *Opt. Commun.*, *210*, 37.
[3] Andreozzi, L., Faetti, M., Giordano, M., Palazzuoli, D., & Galli, G. (2001). *Macromolecules*, *34*, 7325.
[4] Andreozzi, L., Camorani, P., Faetti, M., & Palazzuoli, D. (2002). *Mol. Cryst. Liq. Cryst.*, *375*, 129.
[5] Landraud, N., Peretti, J., Chaput, F., Lampel, G., Boilot, J. P., Lahlil, K., & Safarov, V. I. (2001). *Appl. Phys. Lett.*, *79*, 4562.
[6] Angeloni, A. S., Caretti, D., Laus, M., Chiellini, E., & Galli, G. (1991). *J. Polym. Sci., Polym. Chem. Ed.*, *29*, 1865.
[7] Balke, S. T. (1991). *Chemical analysis (N.Y.)*, *113*, 1.
[8] Meira, G. R. (1991). *Chemical analysis (N.Y.)*, *113*, 67.
[9] Fodor, J. S. & Hill, D. A. (1993). *Macromolecules*, *26*, 5379.
[10] Jackson, C. & Yau, W. W. (1993). *Journal of Cromatography*, *645*, 209.
[11] Gloor, W. (1983). *J. Appl. Polym. Phys.*, *28*, 795.
[12] Billmeyer, F. W. (1984). *Textbook of Polymer Science*, Wiley: New York.
[13] Gloor, W. E. (1978). *J. Appl. Polym. Sci.*, *22*, 1177.
[14] Rogosic, M., Mencer, H. J., & Gomizi, A. (1993). *Eur. Polym. J.*, *32*, 1337.
[15] (1989). In: *Polymer Handbook, 3rd ed.*, Brandrup, J. & Immergut, E. H., (Eds.), John Wiley & Sons: New York.
[16] Fox, T. G. & Flory, P. J. (1950). *J. Appl. Phys.*, *21*, 581.
[17] Fox, T. G. (1956). *Bull. Am. Phys. Soc. [2]*, *1*, 123.